MEDICAL IMAGE SEGMENTATION BASED ON SPATIAL INFORMATION ENTROPY GEODESIC ACTIVE CONTOUR MODEL

Xiang MA[1]*, Zhimin WANG[2], Haibo ZHANG[3], Ronghao ZHANG[4]

This paper presents a novel Geodesic Active Contour (GAC) model based on spatial information entropy for the medical images including bias fields and weak edges. The driving term of this model includes two parts: This spatial information entropy based on image can well describe the gray information in the images and overcome the bias of images; the gradient function of this model can be adaptive to segment the target specific. To enhance algorithm efficiency and stability, this paper employs a binary level set method to implement the entire segmentation process. Experiments demonstrate that the method proposed in this paper achieves excellent segmentation results for grayscale uneven images.

Keywords: geodesic active contour model; spatial information entropy; signed pressure force function

1. Introduction

Geodesic Active Contour (GAC) model [1-6] has been widely applied in image segmentation [7-8]. This type of method has better advantages compared to traditional image segmentation methods. Traditional segmentation methods mainly include edge detection, threshold segmentation, and region growing. This model method is based on variational theory and can effectively utilize mathematical theoretical knowledge to more conveniently and accurately segment target boundaries; At the same time, its segmentation accuracy can reach sub-pixel level.

After a long period of development, the segmentation technology of this model has become very mature, and more segmentation methods have been developed under this model. Although there are many methods in this type of model, it is mainly divided into boundary and region-based segmentation models. Among them, active contour models based on boundaries mainly include Snake model [5] and GAC model; The active contour models based on regions mainly

[1]* Lect., Foundation Department, Engineering University of PAP, China, corresponding author, e-mail: 826245892@qq.com
[2] Assoc. Prof., Foundation Department, Engineering University of PAP, China, e-mail: 18700599850@139.com
[3] Lect., Foundation Department, Engineering University of PAP, China, e-mail: zhbzhbzhb2024@126.com
[4] Ms., College of Equipment Engineering, Engineering University of PAP, China, e-mail: 55219395@qq.com

include Chan-Vese (C-V) model [9], Local Binary Fitting (LBF) model [10-11], and Local Gaussian Distribution (LGD) model [12].

The Snake model defines a parameterized initial closed curve and then drives the contour line to evolve towards the image target boundary under the interaction of internal and external forces in the model. When its energy functional takes a minimum value, the contour curve of the model stops evolving and completes the target segmentation. Although this method is more convenient for image segmentation, it also has some drawbacks: firstly, the model has high requirements for selecting the initial curve. Secondly, the driving force of the evolution curve for the concave areas in the image is insufficient, and it cannot converge to the target boundary. Finally, the model failed to segment images with complex topological structures. Based on the above shortcomings of the Snake model, many researchers have proposed a large number of improved models.

The GAC model segments and extracts target boundaries based on image gradient information, which can easily construct energy functionals and has high segmentation efficiency. This model has good segmentation performance for strong edge target images, but its segmentation performance is not ideal for images with noise, weak boundaries, and boundary leakage, and even fails to segment. Zhang et al. utilize region-based GAC model [13] to address issues such as difficulty in segmenting images with noise, weak boundaries, and boundary leakage in the GAC model. This model replaces the boundary stop function in the original GAC model with a sign pressure function based on global information, which can adaptively shrink or expand the evolution curve and better segment the target image. This model can effectively overcome the effects of noise [14] and weak boundaries, but its segmentation performance for images with uneven grayscale is not ideal.

Many scholars have proposed region-based GAC to address the limitations of boundary-based segmentation models, such as excessive dependence on image gradient information and sensitivity to initial curve selection. Among them, Vese and Chan proposed the C-V model, which is a very classic region-based segmentation model. The C-V model utilizes global information during the segmentation process to find the optimal solution on a global scale. This model has a great degree of freedom in selecting the initial curve and is robust to noise, but it fails to segment images with uneven grayscale.

Li et al. construct the LBF model [10-11] to address the issue that the C-V model cannot overcome the grayscale non-uniformity of images. This model is windowed and localized stem from the C-V model. Due to the slow variation of grayscale information in local areas, this model has overcome grayscale non-uniformity to some extent. However, there are many convolution operations in this model, which leads to low segmentation efficiency.

This article improves the traditional GAC model by introducing spatial information entropy. This article introduces a sign pressure function integrate into information entropy to replace the boundary stop function in traditional GAC models, which can adaptively drive the evolution curve for target segmentation. Due to the fact that spatial information entropy reflects the statistical nature of global information, this model can not only effectively overcome the influence of noise and weak boundaries in images, but also effectively overcome the grayscale non-uniformity of images.

2. Background

V. Caselles et al. proposed the GAC model in 1997, which was a significant breakthrough in the application of Partial Differential Equations in image segmentation. They proposed the energy functional as:

$$E^{GAC} = \int_0^{L(C)} g\left(\left|\nabla I * C\right|\right) \mathrm{d}s \tag{1}$$

In the equation, C represents the closed contour curve, $L(C)$ represents curve length, ∇I expresses image gradient information, and s expresses arc length unit of the curve. $g(\nabla I)$ is a boundary stopping function, defined as follows:

$$g(\nabla I) = \frac{1}{1+\left|\nabla G_\sigma * I\right|^p} \tag{2}$$

$g(\nabla I)$ is the boundary indication function, in the formula, G_σ expresses Gaussian kernel with a standard deviation of σ, $*$ represents convolution, and p is generally taken as 1 or 2. According to the variational method, the evolution equation for level set is as follows:

$$\frac{\partial \varphi}{\partial t} = g\left(\left|\nabla I\right|\right)\left(div\left(\frac{\nabla \varphi}{\left|\nabla \varphi\right|}\right) + \alpha \right) + \nabla g \cdot \nabla \varphi \tag{3}$$

In the equation, $div(\cdot)$ represents the divergence operator, and α is a constant.

Because the GAC model simply utilizes the gradient information in image, when there are noise points in the image, the gradient values of the noise points in the image are infinite, which can cause image segmentation failure. When there are weak boundaries and boundary leaks in the image, the evolution curve is prone to cross the target boundary, causing over segmentation and resulting in segmentation failure.

3. GAC model of Spatial Information Entropy

3.1 Image information entropy

Information entropy [15-16] is a unit of measurement for the amount of information in information theory. It is used to describe the amount of information contained in a system. Due to the existence of units for expressing information content in image processing, such as pixel size, it can be inferred that the concept of information entropy can be introduced into image processing. Its definition in image processing is as follows:

In the image, the local information entropy of pixel $x \in \Sigma$ is:

$$E(x) = -\sum_{w(x-y)} p(I(y)) \log p(I(y)) \tag{7}$$

In the formula, $p\left(I(y)\right) = \frac{1}{2\pi\sigma^2} \exp\left(-\frac{I(y)-f}{2\sigma^2}\right)$ represents a Gaussian function distribution centered around x within the region controlled by the window function [15] $w(x-y)$.

3.2 Spatial Information Entropy Symbol Pressure Function

According to literature [16-17], it is known that the grayscale of most medical images follows a Gaussian distribution [18-20] in local areas. This article studies the grayscale distribution of images locally by introducing a window function. This article constructs a symbol pressure function of spatial information entropy [16] (SIE) to take turns the boundary stopping function in GAC models, as shown below:

$$SIEspf = \frac{\int_\Sigma w(x-y) g\left(E_m(x) - E_b(x)\right) \mathrm{d}y}{\max\left(\left|\int_\Sigma w(x-y) g\left(E_m(x) - E_b(x)\right) \mathrm{d}y\right|\right)} \tag{8}$$

In the formula, $E_b(x) = -p_b(I(y)) \cdot \log\left(p_b(I(y))\right)$ represent the entropy of the background area and $E_m(x) = -p_m(I(y)) \cdot \log\left(p_m(I(y))\right)$ represent the entropy of the target area; Σ is the region of image, $p_b(I(y))$ and $p_m(I(y))$ represent the Gaussian distribution functions in the background and Objectives, respectively, and calculate the posterior probability of each pixel in the background and target regions. The following equation is obtained:

$$p_b\left(I(y)\right) = \frac{1}{2\pi\sigma_b^2} \exp\left(-\frac{\left(I(y) - f_b\right)^2}{2\sigma_b^2}\right), \quad p_m\left(I(y)\right) = \frac{1}{2\pi\sigma_m^2} \exp\left(-\frac{\left(I(y) - f_m\right)^2}{2\sigma_m^2}\right) \tag{9}$$

In formula, f_b, σ_b, and f_m, σ_m represent the grayscale mean and variance of the background area and target. Their expressions are as follows:

$$f_b = \frac{\int_\Sigma w(x-y) I(y) H\left(\varphi(y)\right) dy}{\int_\Sigma w(x-y) H\left(\varphi(y)\right) dy}, \quad f_m = \frac{\int_\Sigma w(x-y) I(y) \left(1 - H\left(\varphi(y)\right)\right) dy}{\int_\Sigma w(x-y) \left(1 - H\left(\varphi(y)\right)\right) dy} \tag{10}$$

$$\sigma_b^2=\frac{\int_\Sigma w(x-y)\left(I(y)-f_b\right)^2 H\left(\varphi(y)\right)dy}{\int_\Sigma w(x-y)H\left(\varphi(y)\right)dy},\ \sigma_m^2=\frac{\int_\Sigma w(x-y)\left(I(y)-f_m\right)^2\left(1-H(\varphi(y))\right)dy}{\int_\Sigma w(x-y)\left(1-H(\varphi(y))\right)dy} \tag{11}$$

According to references [16-17], for images with uneven grayscales, the changes in grayscale in smaller areas can also be approximated as Gaussian distribution. Take a point x on the contour and let Σ_y be the local area controlled by $w(x-y)$ with x as the center. Then, the target area Σ_m and the background area Σ_b are the inner and outer areas of Σ_y divided by the contour line. $E_b(x)$ and $E_m(x)$ represent the information entropy within the background and target regions, respectively. When $x\in\Sigma_b$ is present, according to the concept of information entropy, if $E_b(x)$ takes a smaller value and $E_m(x)$ takes a larger value, then there is $SIEspf>0$, which drives the evolution curve to contract towards the target boundary. When $x\in\Sigma_m$ is present, it can be inferred that $E_b(x)$ takes a larger value while $E_m(x)$ takes a smaller value, resulting in $SIEspf<0$, which drives the evolution curve to expand towards the target boundary. According to the Gaussian distribution of image grayscale in local areas, it can be inferred that the posterior probability in the inner and outer regions divided by the contour line is the highest at 1, and it is approximately obtained when the contour line is at the target boundary. When the contour line approaches the target boundary, there are $E_b(x)\approx 0$ and $E_m(x)\approx 0$, and $SIEspf\approx 0$ can be obtained, which causes the evolution curve to stop evolving at the target boundary.

According to formula (8), the range of variation for $SIEspf$ is $[-1,1]$. Based on the above discussion, function $SIEspf$ satisfies the definition of a sign pressure function. At the same time, a spatial function $g(\nabla I)$ is introduced into this symbol pressure function. When the contour curve evolves to the target boundary, the image gradient tends to infinity, forcing the contour curve to stop evolving. This can correct the excessive segmentation caused by the excessive evolution of the contour line. Thereby improving the segmentation accuracy.

3.3 Gradient Descent Flow Equation

The GAC model of Spatial Information Entropy (SIE-GAC), by replacing $g(\nabla I)$ in the original GAC model with $SIEspf$, obtains the corresponding equation as follows:

$$\frac{\partial\phi}{\partial t}=SIEspf\cdot|\nabla\phi|\cdot\left[div\left(\frac{\nabla\phi}{|\nabla\phi|}\right)+\alpha\right]+\nabla SIEspf\cdot\nabla\phi \tag{12}$$

It can be seen that the symbol pressure function in this article is based on spatial information entropy, which depends on global statistical information in image. According to references [16-17], it is known that in medical images, if the grayscale values in a small neighborhood change slowly, then the derivative of $SIEspf$ can be approximated as zero, that is $\nabla SIEspf \approx 0$. Meanwhile, in this article, $div\left(\frac{\nabla\phi}{|\nabla\phi|}\right)\cdot|\nabla\phi|$ is referred to as $\Delta\phi$, which can be approximated by $G_\sigma * \phi$ applying Gaussian filtering smoothing to the curve, thus replacing the role of curvature regularization term. As can be seen from the above, equation (12) can be simplified as:

$$\frac{\partial\phi}{\partial t} = \alpha \cdot sespf \cdot |\nabla\phi| \quad (13)$$

In this article, the gradient descent flow equation [21-22] is concise and effective, while avoiding a large number of convolution operations and improving computational efficiency. In addition, this method can better distinguish between background and target, resulting in ideal image segmentation results. Compared to the sign pressure function that utilizes global information, the sign pressure function based on local information entropy introduces a window function and utilizes the local statistical information of the image to better reflect the grayscale changes of the image. Compared to edge stopping functions, it is better suited for segmenting targets with noise or weak boundaries.

4. Experimental Results and Analysis

This experiment is implemented using MATLAB software with a time step of $t = 0.1s$. In the experiment, the $w(x-y)$ uses a Gaussian template of size $(4m+1)\times(4m+1)$, and the size of the Gaussian smoothing template is $k\times k$, where k takes the value of $(3, 9)$ and the standard deviation σ ranges from $(3, 21)$. Adjust parameter α appropriately according to different images.

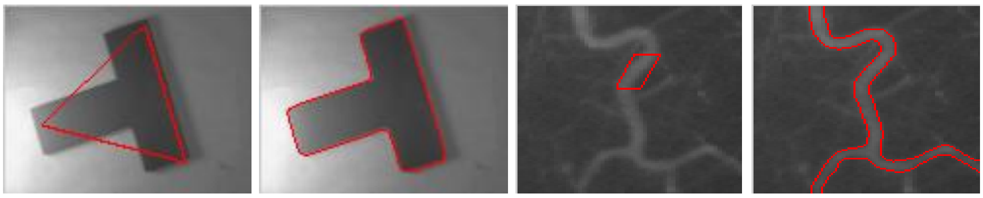

Fig.1. The segmentation effect of images using the method described in this article.

Fig. 1 shows the experimental segmentation effect of synthetic image and real vascular image. Among them, Fig. 1a and Fig. 1c are the original images and initial contour lines; Figs. 1b and 1d show the experimental results of the method proposed in SIE-GAC. From the synthesized images and real vascular maps, it can be seen that these images contain noise, weak boundaries, uneven grayscale, and complex topological structures. However, the method proposed in SIE-GAC achieved good experimental results, indicating that it has good segmentation performance for images with noise, weak boundaries, and grayscale non-uniformity.

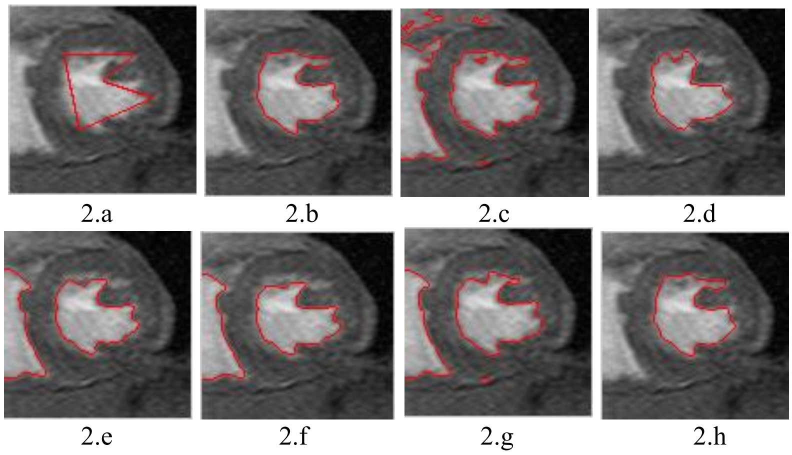

Fig. 2. Experimental segmentation results of left ventricular images

Figs. 2.a-b show the left ventricular magnetic resonance images, initial contour lines, and standard segmentation results; Figs. 2.c-h show the experimental results of different models. Fig. 2.c shows the experimental results of the C-V model, which is based on global information and has good segmentation performance for noisy images, but fails to segment images with uneven grayscale. Fig. 2.d shows the experimental effect of the GAC model after 400 iterations，this method has good segmentation results for strong edge targets, but fails to segment images containing noise, weak boundaries, and uneven grayscale. Fig. 2.e shows the experimental effect of the region-based GAC model after 100 iterations, which can be affected by noise and grayscale unevenness, but the segmentation results are not very ideal. Fig. 2.f shows the experimental effect of the LBF model after 100 iterations with parameters $\lambda_1 = 1.0$ and $\lambda_2 = 1.0$, kernel parameter sigma=15. Although this model effectively overcomes the impact of uneven grayscale, it is based on local regions of the image and is prone to getting stuck in local optima, leading to over segmentation. Fig. 2.g shows the experimental results of LGD model with parameters $\lambda_1 = 1.0$ and $\lambda_2 = 1.0$, and kernel parameter sigma=15 for 200 iterations. This model effectively overcomes grayscale unevenness but fails to segment noisy points. Fig. 2.h shows the segmentation results based on the SIE active contour model in SIE-GAC. The SIE in this method can better describe the grayscale information distribution of the image and effectively segment the target boundary.

For the sake of reflecting and comparing the segmentation precision and time efficiency of various models, we conducted segmentation experiments using 20 sets of left ventricular grayscale images with a size of 110×110. We also used the Jaccard Similarity (JS) index [23] to quantitatively analysis the accuracy of the experimental results.

According to the experimental effect, the segmentation precision of SIE-GAC is over 90%, which is superior to other models in this paper. The C-V model utilizes the grayscale to mean information of images and has good robustness to images containing noise, blurred or fractured boundaries, but fails to segment images with uneven grayscale. The GAC model utilizes image gradient information and has good segmentation performance for strong edge target boundaries. However, it is prone to getting stuck in local optima at noisy points, and when there are weak or blurry boundaries in the image, boundary leakage is likely to occur. The region-based GAC model utilizes a sign pressure function based on global information to achieve good segmentation results for targets with noise and weak boundaries, but it is prone to over segmentation of homogeneous regions. The LBF model and LGD model utilize local information of the image, which can effectively overcome grayscale non-uniformity. However, due to the large number of convolution operations, the segmentation efficiency is reduced. This article uses spatial information entropy to better describe the global grayscale information of an image, while also effectively overcoming grayscale non-uniformity. In this method, window convolution calculation is used. Although it increases the segmentation time and iteration times, the average segmentation time is less than 3 seconds and the iteration count are less than 200, which is still within a reasonable range.

Table 1

Comparisons of JS value and segmentation rate of different models

Algorithm	Iteration count	Segmentation accuracy	Segmentation time
CV	400	0.4872	23.039351
GAC	400	0.7771	5.863287
LBF	100	0.5326	18.028198
LGD	200	0.5444	10.715657
region-based GAC	100	0.5326	0.641432
Proposed Method	150	0.9591	2.723898

The iteration times, average segmentation time, and average segmentation accuracy values of the various segmentation methods mentioned above are shown in Table 1.

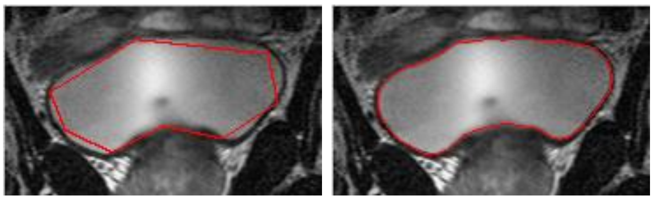

3.a 3.b

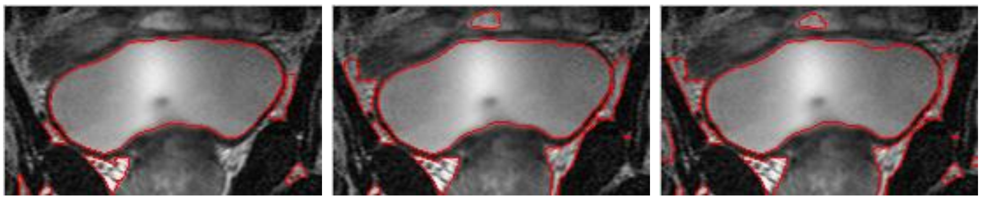

3.c(1) 3.c(2) 3.c(3)

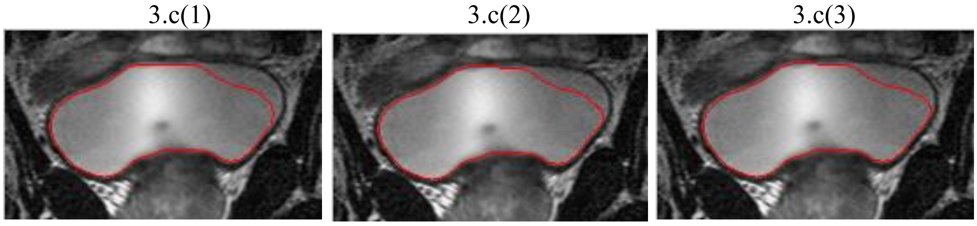

3.d(1) 3.d(2) 3.d(3)

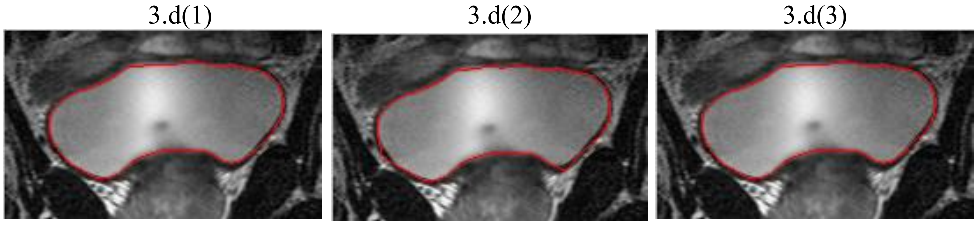

3.e(1) 3.e(2) 3.e(3)

Fig.3. Segmentation results of ultrasound images when sigma is 3, 9, 15

Fig. 3 shows a comparison of segmentation effects of different models on ultrasound images with different values of σ and $\alpha = 3$. Fig. 3.a shows the original image and initial curve, Fig. 3.b shows the accurate segmentation results, Figs. 3.c(1) to 3.c(3), Figs. 3.d(1) to 3.d(3), and Figs. 3.e(1) to 3.e(3) respectively show the segmentation results of the region-based GAC model, LBF model, and the methods in this paper when the kernel parameter sigma size is [3,9,15].

Fig. 4.a-c shows the impact of different values of parameter $\alpha = [3,6,9]$ on the segmentation results in this article.

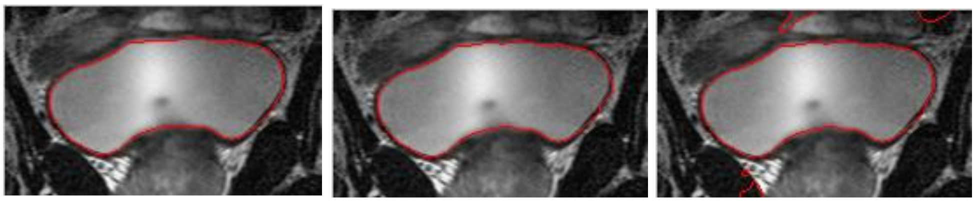

Fig.4. The effect of alpha by segmentation results in this method

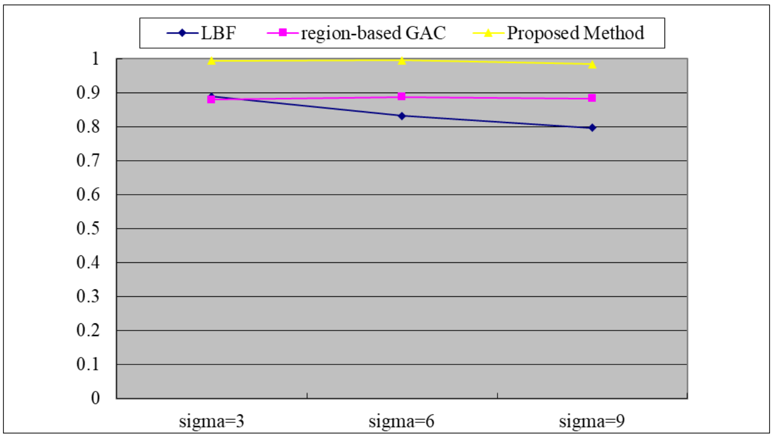

Fig.5. The influence of kernel parameter sigma on segmentation accuracy

Fig. 5 shows the impact of the kernel parameter sigma size on image segmentation accuracy in Fig. 3. From Fig. 5, it can be seen that the method proposed in SIE-GAC is significantly superior to the LBF model and the region-based GAC model and has a good effect on overcoming noise and grayscale non-uniformity, accurately segmenting images, and improving the robustness of kernel parameters.

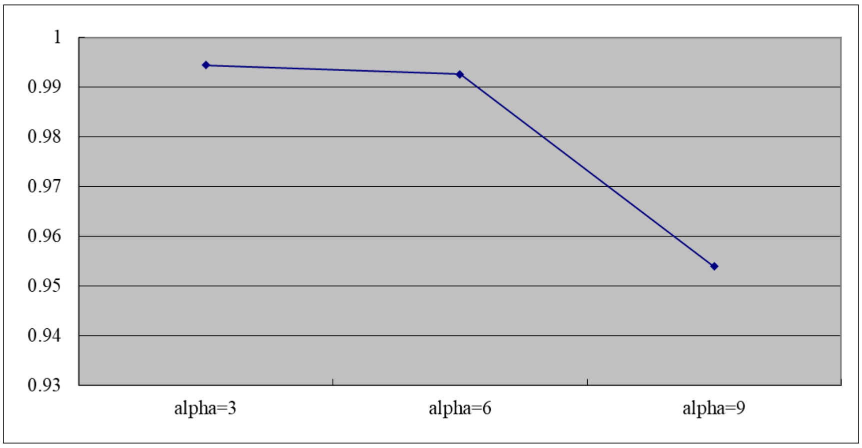

Fig.6. The effect of alpha by JS values in this method

Fig. 6 shows the impact of parameter α variation on segmentation accuracy. The parameter α in this method achieves good segmentation results within the range of intervals [3, 6]. As shown in this figure, the selection requirements for parameter α in this method are relatively high. When the value of parameter α is large, it can lead to inaccurate segmentation of the target boundary or cause over segmentation.

5. Conclusions

This paper proposes an improved GAC model to address the common phenomena of noise, offset fields, and weak boundaries in images. SIE-GAC proposes a symbol pressure function based on spatial information entropy, utilizing the global information of the image to effectively overcome grayscale non-uniformity. Meanwhile, the model also has good segmentation performance containing noise and weak boundaries. Compared with the GAC model, this method has higher segmentation efficiency and can prevent weak boundary leakage. Compared with the C-V model and the region-based GAC model, the method proposed in SIE-GAC can better overcome grayscale non-uniformity. Relatively speaking, the kernel parameter selection of this paper method has a larger space exceeding LBF and LGD model.

R E F E R E N C E S

[1]. *Tushar Saini*, *Panos S. Shiakolas*, “In Situ Active Contour-Based Segmentation and Dimensional Analysis of Part Features in Additive Manufacturing”, in Journal of Manufacturing and Materials Processing, **vol. 3**, no. 9, Mar, 2025, pp. 1-26

[2]. *Vincent Majanga*, *Ernest Mnkandla, et al.*, “Active Contours Connected Component Analysis Segmentation Method of Cancerous Lesions in Unsupervised Breast Histology Images”, in Bioengineering, **vol. 6**, no. 12, Jun., 2025, pp. 1-21

[3]. *Miguel Chicchon*, *Francesca Colosi, et al.*, “Urban Sprawl Monitoring by VHR Images Using Active Contour Loss and Improved U-Net with Mix Transformer Encoders”, in Remote Sensing, **vol. 9**, no. 17, Apr., 2025, pp. 1-22

[4]. *Suane Pires Pinheiro da Silva*, *Roberto Fernandes Ivo, et al.*, “Context-Driven Active Contour (CDAC): A Novel Medical Image Segmentation Method Based on Active Contour and Contextual Understanding”, in Sensors, **vol. 9**, no. 25, Apr., 2025, pp. 1-41

[5]. *Xiaoyu Pan*, *Delun Wang,* “GC Snakes: An Efficient and Robust Segmentation Model for Hot Forging Images”, in Sensors, **vol. 15**, no. 24, Jul., 2024, pp. 1-28

[6]. *Yangyang Song, Guahua Peng, et al.* “Active contours driven by Gaussian function and adaptive-scale local correntropy-based K-means clustering for fast image segmentation”, in Signal Processing, **vol. 174**, Sep., 2020, pp. 1-14

[7]. *Eduardo Galicia Gómez*, *Fabián Torres-Robles, et al.,* “A Shape Regression Convolutional Neural Network Ensemble Applied to the Segmentation of the Left Ventricle in Echocardiography”, in Journal of Imaging, **vol. 5**, no. 11, Jul, 2025, pp. 1-22

[8]. *Shuwang Zhou*, *Minglei Shu, Chong Di,* “A Multi-Source Circular Geodesic Voting Model for Image Segmentation”, in Journal of Imaging, **vol. 12**, no. 26, Dec., 2025, pp. 1-23

[9]. *T.Chan*, *L.Vese*, “Active contours without edges”, in IEEE Transactions on Image processing, **vol. 10**, no. 2, Feb., 2001, pp. 266-277

[10]. *Yangyang Song, Guahua Peng,* “Improving the Convergence of Local Binary Fitting Energy for Image Segmentation”, International Conference on Graphics and Image Processing, **vol. 11069**, May, 2019.

[11]. *Dansong Cheng, Daming Shi, et al.* “A level set method for image segmentation based on Bregman divergence and multi-scale local binary fitting”, in Multimedia Tools and Applications, **vol. 4**, no. 15, Mar,2019. pp.20585–20608

[12]. *Li Wang, Lei He, et al*., “Active contours driven by local Gaussian distribution fitting energy”, in Signal Processing, **vol. 12**, no. 89, 2009, pp. 2435-2447
[13]. *Kai hua Zhang, Lei zhang, et al*. “Active contours with selective local or global segmentation: A new formulation and level set method”, in Image and Vision computing, **vol. 28**, no. 4, 2010, pp. 668-676
[14]. *Michael Peleg*, *Shlomo Shamai,* “Geometry-Based Bounds on the Capacity of Peak-Limited and Band-Limited Signals over the Additive White Gaussian Noise Channel at a High SNR”, in Entropy, **vol. 12**, no. 27, Nov., 2025, pp. 1-20
[15]. *Zichuan Fu, Wentao Song, et al*. “Sliding Window Attention Training for Efficient Large Language Models”, in arXiv:2502.18845 [cs.CL], Feb, 2025, pp.1-14
[16]. *Jianwei Zhang, Xiang Ma, et al*. “Image Segmentation Based on Local Information Entropy Geodesic Active Contour Model”, in International Journal of Multimedia Ubiquitous Engineering, **vol. 4**, no. 9, 2014, pp.127-136
[17]. *Daniel E. Clark,* “Local Entropy Statistics for Point Processes”, in IEEE Transactions on Information Theory, **vol. 66**, no. 2, Feb, 2020, pp. 1155-1163
[18]. *Wenwen Hu*, *Kaitai Fang, Xiaoling Peng,* “Representative Points of the Inverse Gaussian Distribution and Their Applications”, in Entropy, **vol. 12**, no. 27, Nov, 2025, pp. 1-28
[19]. *Kaitai Fang*, *Yuxuan Lin, Yuhui Deng,* “A Review: Construction of Statistical Distributions”, in Entropy, **vol. 12**, no. 27, Nov, 2025, pp. 1-36
[20]. *Alex Dytso, Ronit Bustin, et al*. “Analytical properties of generalized Gaussian distributions”, in Journal of Statistical Distributions and Applications, **vol. 5**, no. 6, Dec, 2020, pp. 1-40
[21]. *Sanjeev Arora, Zhiyuan Li, Abhishek Panigrahi,* “Understanding Gradient Descent on the Edge of Stability in Deep Learning”, in 39th International Conference on Machine Learning, **vol. 162**, 2022, pp.948-1024
[22]. *Christopher M De Sa, Satyen Kale, et al*. “From Gradient Flow on Population Loss to Learning with Stochastic Gradient Descent”, in Neural Information Processing Systems 35 (NeurIPS 2022), 2022, pp.1-14
[23]. *Gonzalo Travieso, Alexandre Benatti and Luciano da F. Costa,* “An Analytical Approach to the Jaccard Similarity Index”, in arXiv:2410.16436 [physics.data-an], Oct, 2024, pp.1-17